Directional acoustic response of a silicon disc-based microelectromechanical systems structure

David James Mackie[1], Joseph Curt Jackson[1], James Gordon Brown[2], Deepak Uttamchandani[2], James Frederick Charles Windmill[1]

[1]*Department of Electronic and Electrical Engineering, Centre for Ultrasonic Engineering, University of Strathclyde, Glasgow G1 1XW, United Kingdom*
[2]*Department of Electronic and Electrical Engineering, Centre for Microsystems and Photonics, University of Strathclyde, Glasgow G1 1XW, United Kingdom*
E-mail: david.mackie@strath.ac.uk

Published in Micro & Nano Letters; Received on 14th November 2013; Revised on 12th March 2014; Accepted on 21st March 2014

A microelectromechanical systems (MEMS)-based structure capable of operating mechanically as a directional acoustical sensor is presented. The structure, fabricated through the commercially available SOIMUMPS foundry process, consists of two circular discs attached to a central suspension beam, fixed at both ends. The design of the structure resembles other directional MEMS microphones that mimic the directional hearing organ of the parasitoid fly, *Ormia ochracea*. Modal analysis and mechanical acoustic directionality analysis using both laser Doppler vibrometry and finite element modelling have been implemented. It is demonstrated that this coupled MEMS structure exhibits an acoustic directional response, with a one-to-one relationship between the relative vibration amplitudes of the two coupled discs and the angle of sound, from −75° to +60°.

1. Introduction: Microelectromechanical systems (MEMS) microphones are becoming increasingly common in portable devices such as hearing aids, smartphones and tablet computers, among other applications [1, 2]. Several advantages lie in using a MEMS device, notably size and the integration of electronic functionality such as filtering and amplification. In addition, the robust mechanical properties of silicon make it ideal for the demanding conditions experienced in the above applications [3]. Although MEMS technology has been applied in commercial microphones, achieving directionality within such devices is currently a subject of the research domain. The inclusion of directionality in a microphone system can provide an approach to reducing noise and thus promoting signal intelligibility, for example, in speech, or the ability to accurately locate sound sources, such as in environmental monitoring [4–6]. However, there are physical constraints to designing a directional microphone.

Traditional directionality (extending to localisation in three dimensions) in conventional microphone systems usually involves an array of two or more pressure receivers, whose separation is greater than the wavelength of the incident sound. Such systems use an estimate of the time difference of arrival (TDOA), or a relative phase difference, and sometimes the difference in sound intensity at each receiver as inputs to algorithms which compute the location of the sound source. When miniaturising such directional microphone systems, a problem arises as the separation between receivers becomes smaller than the wavelength of incident sound, such that the TDOA and pressure difference measurements become less accurate, leading to greater errors in source localisation. For example, the typical acoustic wavelength for audio applications is of the order of centimetres, therefore imposing a size constraint on the miniaturisation of traditional directional receiver arrays.

Inspiration for silicon MEMS-based directional microphones has often been taken from the unique directional hearing system observed in the parasitoid fly, *Ormia ochracea* [1, 7–12]. The *Ormia* deposits its eggs on and around a singing male cricket, which is then used as a food source by the larvae. The fly locates the cricket by localising the cricket's acoustic signal (song) with accuracy better than 2°. The pressure receivers, specifically the tympanal membranes, within the *Ormia* ear are separated by just 0.5 mm, yet the cricket host's calling song has a wavelength of the order of centimetres. A mechanical coupling arrangement between the pair of tympanal membranes, namely the intertympanal bridge, causes the combination of two major modes of vibration which, favourably for the fly, results in a significant amplification of the perceived pressure intensity difference. The two modes are usually described as a 'rocking' mode, where the two membranes deflect 180° out of phase, and a 'translational' in-phase mode [12, 13].

Several previous studies have applied MEMS technology to mimic the dynamics of the ear of *Ormia* [1, 7–12]. While various degrees of success have been reported, directional acoustic sensitivity should, in principle, be present in any micromechanical device with sufficient degrees of freedom of movement. In this Letter, we present findings on the directional response of a simple, single-crystal silicon MEMS structure that is similar in size and geometry to the fly ear, and the several bio-inspired directional MEMS microphones which have been previously reported. The modal analysis of the structure and its performance, mechanically, as a directional acoustic sensor are investigated both experimentally and computationally. The structure exhibits acoustic directionality, demonstrating the potential for such micromechanical devices to be utilised as directional microphones.

2. Methods: The MEMS structure consists of two circumferentially unclamped circular plates, each 1000 µm in diameter and 10 µm in thickness, which are directly attached to a suspension beam 3000 µm long, 40 µm wide and 10 µm thick, anchored at both ends. Fig. 1*a* shows a scanning electron micrograph (SEM) of the structure. The defining dimensions are shown clearly in Fig. 1*b*, created using SolidWorks three-dimensional (3D) CAD software (Dassault Systèmes SolidWorks Corp., Waltham, MA, USA). This structure was fabricated using a commercial multi-user silicon-on-insulator process (SOIMUMPs) offered by MEMSCAP Inc., Durham, NC, USA [14]. The starting substrate consists of a 10 µm layer of single-crystal silicon, attached to a 400 µm-thick handle wafer by an oxide layer of thickness 1 µm. Two methods are then used during the fabrication of the MEMS structure – patterning and etching of the silicon wafer from the top surface down to the

doi: 10.1049/mnl.2013.0677

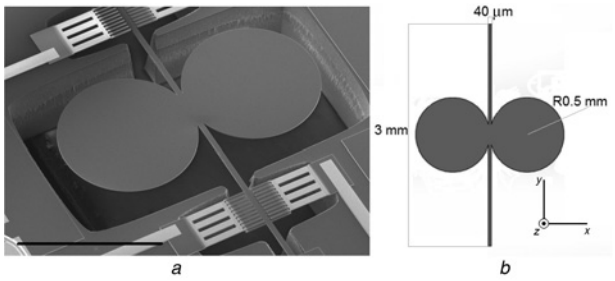

Figure 1 *Silicon MEMS structure*
a Scanning electron micrograph of the MEMS device (scale bar represents 1 mm)
b Dimensioned 3D CAD model of the device using SolidWorks

oxide layer, and patterning and etching through the bottom surface of the handle wafer substrate to the oxide layer.

2.1. Laser Doppler vibrometry (LDV): Modal analysis was carried out by observing the vibration of the structure with micro-scanning LDV, in response to various acoustic stimuli. LDV measures the structure's out-of-plane vibration velocity. The structure was located off-centre on a 11 mm × 11 mm die of thickness 400 µm fixed onto a 70 mm × 28 mm × 2.5 mm printed circuit board (PCB), with a centrally cut hole in the PCB exposing the bottom face of the structure. This enabled access to both sides of the mounted structure. The orientation of the structure was with the *xz* plane parallel to the floor and the *y*-axis perpendicular to the floor, according to Fig. 1*b*.

The scanning laser vibrometer (Polytec PSV-300-F; Waldbronn, Germany) has an OFV-056 scanning head and close-up attachment fitted yielding a positioning accuracy of 1 µm and spot diameter 5 µm. The vibrating surface of the structure was measured in steps of 50 µm. Acoustic frequency signals were generated [Agilent 33220A; Santa Clara, USA)], amplified (Sony TA-FE570; Tokyo, Japan) and passed to a loudspeaker (ESS Heil Air Motion Transformer; South El Monte, USA), positioned 500 mm from the structure. A precision pressure microphone (Brüel & Kjær 4138; Nærum, Denmark) connected to a pre-amplifier (Brüel & Kjær Nexus 2690; Nærum, Denmark) measured the sound pressure approximately 10 mm from the structure and was used to provide a reference signal for the vibrometer. Initially the acoustic signal generated consisted of wideband chirps of frequency range 1–25 kHz, to determine the frequency response of the structure. Modes identified during this process were subsequently investigated with single frequency pure tones to excite the mode and record an accurate mode shape.

Directional analysis involved the measurement of the velocity of the outer edge of each disc in response to a 1.2 kHz pure tone sound stimulus. The frequency was selected based on the modal analysis results, such that while it is relatively close to mode resonance frequencies, it is not a frequency corresponding to a specific mode (see Section 3). The position angle, θ, defined in the *xz* plane, is the angle between the loudspeaker and the *z*-axis. This angle was varied from −90° (closest to the right disc) through 0° (normal to the structure) to +90°, in 5° steps. Post-processing of this data using the fast Fourier transform with a rectangular window allowed computation of the transfer function of the structure velocity to sound pressure level (Pa). From this the amplitude gain in m/s/Pa was calculated (ratio of structure velocity to sound pressure). At each θ, the amplitude gain of the edge of the right-hand and left-hand discs was measured. The directional intensity gain was then defined as the ratio of these two amplitude gains.

2.2. Finite element modelling: COMSOL multiphysics was used to simulate the response of the MEMS structure. Modal analysis was implemented through eigenfrequency studies of a 3D finite element model (FEM) of the structure. This computes the undamped, unforced modes of vibration of the MEMS structure. The geometry was built within COMSOL's environment and two executions were run using different material model types. The first assumes purely isotropic silicon of density 2330 kg/m^3, Young's modulus 131 GPa and a Poisson's ratio of 0.27. In the second execution anisotropic single-crystal silicon was used allowing for the directional variation in the Young's modulus. The first six eigenmodes of each of these models were computed.

For computational directionality analysis, the structure, including the surrounding die, was modelled, with the hole behind the structure and a surrounding air domain incorporated. The material model type was the anisotropic silicon complete with crystal rotation, that is, the second setup mentioned previously. By coupling both the fields of acoustics and structural mechanics, an acoustic–structure interaction computes the two-way interaction between the mechanical response of a structure and an incident pressure wave in the surrounding fluid domain. An incident plane wave pressure field of amplitude 0.06 Pa (∼70 dB sound pressure level re 20 µPa) was used in the model and, to match the experimental studies, an operating frequency of 1.2 kHz was chosen. By parameterising the defining angles of the load pressure wave, a double parametric sweep was executed allowing efficient calculation of the response of the structure at each angle, θ, required. Importantly, the geometric nonlinearity feature was enabled as a study setting because of the nature of the suspension beam in the structure.

Post-processing within COMSOL allowed the extraction of displacements and velocities (and other characteristics) at user-defined points on the structure such that the directional intensity gain, as defined in the laser vibrometry section 2.1 above, could be calculated for each angle of sound source, θ.

3. Results

3.1. Modal frequency analysis – measured against simulated: Fig. 2 shows the shape of the four out-of-plane modes of vibration found between 1 and 21 kHz using both finite element modelling (left) and laser vibrometry (right). Complementing this Figure is Table 1, collating the detected modes of vibration in both the experiment and the simulation. Analysis of the laser vibrometry data shows that the first mode of vibration is found at around 1.40 kHz. This mode can be described as a rotational mode with the suspension beam as the axis of rotation, that is, both discs moving 180° out of phase of each other, resulting in a so-called rocking mode. Executing an eigenfrequency study of the FEM of the structure, treating the silicon simply as an isotropic material, yields the rocking mode at 1.44 kHz (Table 1).

Eigenmode analysis of a FEM with a material model that includes the anisotropy of silicon yielded the first mode as the rocking mode at a frequency of 1.45 kHz.

Experimentally, the structure had a translational mode at 2.20 kHz and at this mode of vibration the structure appears to be more sensitive than at the lower frequency rocking mode (see the difference in the range of gain in Figs. 2*b* and *d*). This piston mode is found to have a frequency of 1.62 and 1.83 kHz for the isotropic model and the anisotropic model, respectively.

The correlation between the vibrometry results and the FEM results appears to be extremely strong for the model with anisotropic

Table 1 Modal frequencies of the structure calculated using vibrometry and finite element modelling

Mode		Modal frequency, kHz					
		First	Second	Third	Fourth	Fifth	Sixth
LDV experiment		1.40	2.20	7.39	NA	NA	20.51
FEM	Iso Si model	1.44	1.62	5.82	6.64	9.91	18.41
	Aniso Si model	1.45	1.83	6.56	7.50	11.16	20.64

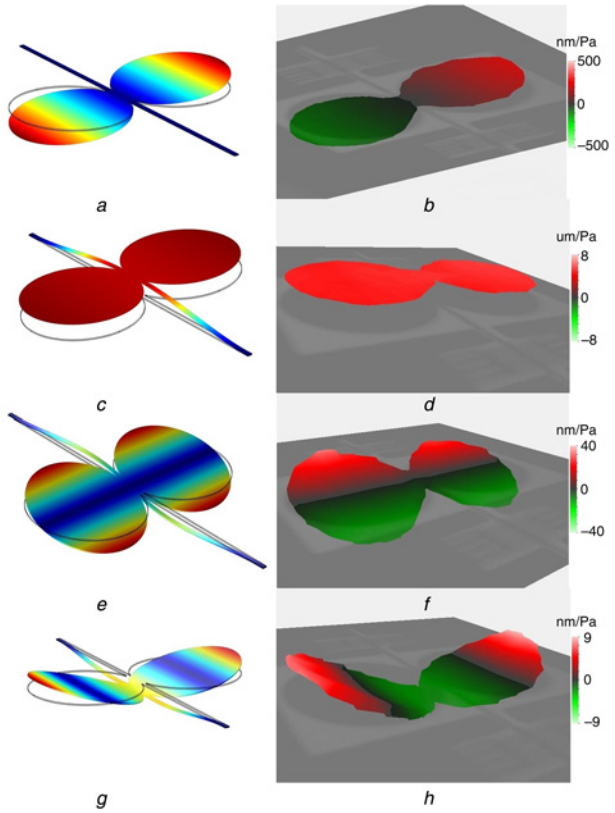

Figure 2 *First four out-of-plane mode shapes of the device*
a FEM simulated first (rocking) mode
b LDV measured first mode
c Second (translational) mode through FEM simulation
d Second mode as observed using LDV
e FEM computed third mode
f LDV measured third mode
g Fourth (flapping) mode as computed by FEM
h Fourth mode captured using LDV

Si combined with a rotation of the geometry within the workspace. Table 1 shows that this correlation continues across all four out-of-plane modes found during modal analysis using LDV, that is, rows 1 and 3 correlate well.

The third mode of vibration of the structure, described as a rotational mode with the axis of rotation through the centre of the two circular discs, is found to have a frequency of 7.39 kHz (LDV) and 6.56 kHz (FEM). Likewise, for the sixth mode, described as a flapping mode (see Figs. 2*g* and *h*), vibrometry shows it to have a frequency of 20.51 kHz and the model predicts a frequency of 20.64 kHz.

Modes four and five are in-plane twisting and in-plane bending modes which are undetectable using LDV in this way, since

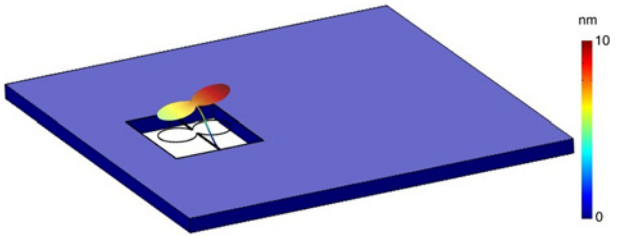

Figure 3 *Finite element analysis of the device using COMSOL's acoustic–structure interaction*
Incident sound is a plane wave of frequency 1.2 kHz, sound level of 0.06 Pa at an angle 20° to the normal from left to right
Instantaneous displacement of the device ranges from 5 to 10 nm at this moment in the cycle, whereas the die remains stationary in comparison

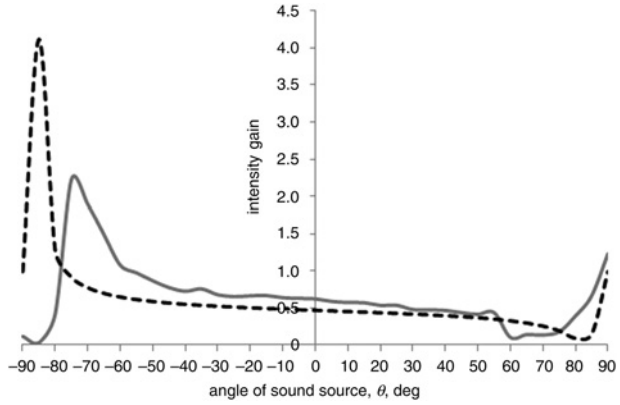

Figure 4 *Directional intensity gain (solid grey line) against sound source angle, θ, calculated from LDV data*
Broken black line is directional intensity gain against sound source angle, θ, computed using COMSOL Multiphysics
From approximately −75° to +60°, there is a one-to-one relationship between the relative vibration amplitudes of each disc and the angle of incidence

when vibrating in these modes the structure has no out-of-plane velocity component.

3.2. Directionality analysis: Laser vibrometry was also used to analyse the directionality of the structure as described in Section 2. Plotting the intensity gain calculated from vibrometer data against the angle of sound source, θ, results in the solid grey line shown in Fig. 4.

This experiment is repeated computationally as an acoustic–structure interaction in the frequency domain with COMSOL, as outlined in Section 2, using nested parametric sweeps to simulate all the same sound source angles (θ) used in the vibrometry measurements. Fig. 3, in which the vertical scale is multiplied by a factor of 1.5×10^5, shows a snapshot of the dynamic cycle of the simulated structure and die in response to a pure tone sound stimulus of 1.2 kHz, at a sound level of 0.06 Pa, at $\theta = +20°$. The deflection of the structure clearly displays a combination of both the rocking and translational modes, with a maximum displacement of 10 nm at the instant the snapshot was taken.

The broken black line in Fig. 4 represents the data from this FEM simulation, and displays a similar relationship to that observed from the LDV results. Both results display similar distinctive characteristics in that the intensity gain, or intensity ratio of the right disc to left disc, reaches a maximum at a large negative sound source angle θ, −85° for the model where the gain is 4, and −70° in LDV where the gain is between 2 and 2.5. Similarly the gain converges to a minimum of 0.1 at a high positive stimulus angle θ, 80° and 60° from FEM and LDV, respectively. Both the vibrometry and the modelling results display a gain of about 0.5 when the sound source is at $\theta = 0°$, or normal to the structure. A possible explanation for the relative difference in the position of maxima and minima between the experimental and simulated results is that while the simulation assumes a free-field, in the experiment various apparatus surrounds the device, for example, the laser vibrometer and fixtures for mounting the device.

4. Conclusion: A single-crystal silicon MEMS structure, consisting of two circular discs connected to a centrally supporting beam, has been fabricated using commercially available SOIMUMPs. Using both LDV and FEM to investigate the natural modes of vibration of the structure has resulted in observation of the same first four out-of-plane mode shapes. There is also close correlation between measured frequencies through both methods, particularly when correctly allowing for the anisotropy of single-crystal silicon. This is without consideration of damping characteristics. However, because the

doi: 10.1049/mnl.2013.0677

removal of a section of the PCB fully exposed the posterior surface of the structure, then a major contribution to damping in many MEMS structures of this style – squeeze-film damping – is eliminated.

When stimulated at an appropriate frequency, the structure appears to exhibit an interaction between two, spectrally close, modes called rocking and translational, which combine in differing proportions dependent on the angle of the sound source. The outcome of this effect is a predictable and repeatable relationship between the directional intensity gain and the angle of source. Both FEM simulations and LDV experimentation confirm this relationship. Therefore the structure is capable of performing as a directional microphone because of the coupling of two natural modes of vibration whose resonance frequencies are close.

The extent of how successfully this structure performs in terms of mechanical directionality may well be limited by the relative sensitivity of the structure to both the translational mode and rocking mode, that is, the translational mode somewhat dilutes the influence of the rocking mode, resulting in a sub-optimal mechanical directionality performance.

The simple MEMS structure presented here, while resembling biologically inspired microphones, was not optimised. However, it exhibits acoustic directionality, indicating that a variety of simple MEMS devices could have acoustic directionality not apparent during design or experimental characterisation, thus demonstrating the potential for such micromechanical devices to be utilised as directional microphones.

5. Acknowledgments: This work was supported by the Biotechnology and Biological Sciences Research Council, UK (grant BB/H004637/1), and the Engineering and Physical Sciences Research Council, UK (EP/H02848X/1).

6 References

[1] Miles R.N., Hoy R.R.: 'The development of a biologically inspired directional microphone for hearing aids', *Audiol. Neurootol.*, 2006, **11**, (2), pp. 86–94

[2] Wang W.J., Lin R.M., Zou Q.B., Li X.X.: 'Modeling and characterization of a silicon condenser microphone', *J. Micromech. Microeng.*, 2004, **14**, pp. 403–409

[3] Scheeper P.R., van der Donk A.G.H., Olthuis W., Bergveld P.: 'A review of silicon microphones', *Sens. Actuators A, Phys.*, 1994, **44**, (1), pp. 1–11

[4] Ricketts T.A.: 'Impact of noise source configuration on directional hearing aid benefit and performance', *Ear Hear*, 2000, **21**, (3), pp. 194–205

[5] Gnewikow D., Ricketts T., Bratt G.W., Mutchler L.C.: 'Real-world benefit from directional microphone hearing aids', *J. Rehab. Res. Dev.*, 2009, **46**, (5), pp. 603–618

[6] Blumstein D.T., Mennill D.J., Clemins P., *ET AL.*: 'Acoustic monitoring in terrestrial environments using microphone arrays: applications, technological considerations and prospectus', *J. Appl. Ecol.*, 2011, **48**, (3), pp. 758–767

[7] Yoo K., Gibbons C., Su Q.T., Miles R.N., Tien N.C.: 'Fabrication of biomimetic 3D structured diaphragms', *Sens. Actuators A, Phys.*, 2002, **97–98**, pp. 448–456

[8] Liu H.J., Yu M., Zhang X.M.: 'Biomimetic optical directional microphone with structurally coupled diaphragms', *Appl. Phys. Lett.*, 2008, **93**, (24), p. 243902

[9] Touse M., Sinibaldi J., Simsek K., Catterlin J., Harrison S., Karunasiri G.: 'Fabrication of a microelectromechanical directional sound sensor with electronic readout using comb fingers', *Appl. Phys. Lett.*, 2010, **96**, (17), p. 173701

[10] Lisiewski A.P., Liu H.J., Yu M., Currano L., Gee D.: 'Fly-ear inspired micro-sensor for sound source localization in two dimensions', *J. Acoust. Soc. Am.*, 2011, **129**, (5), p. EL166–71

[11] Chen C., Cheng Y.: 'Physical analysis of a biomimetic microphone with a central-supported (C-S) circular diaphragm for sound source localization', *IEEE Sens. J.,* 2012, **12**, (5), pp. 1504–1512

[12] Miles R.N., Robert D., Hoy R.R.: 'Mechanically coupled ears for directional hearing in the parasitoid fly *Ormia ochracea*', *J. Acoust. Soc. Am.*, 1995, **98**, (6), pp. 3059–70

[13] Robert D., Miles R.N., Hoy R.R.: 'Tympanal mechanics in the parasitoid fly *Ormia ochracea* : intertympanal coupling during mechanical vibration', *J. Compar. Physiol. A, Sens. Neural Behav. Physiol.*, 1998, **183**, (4), pp. 443–452

[14] Cowen A., Hames G., Monk D., Wilcenski S., Hardy B.: 'SOIMUMPs design handbook' (2011, 8th edn), http://www.memscap.com/products/mumps/soimumps/reference-material.htm, accessed 5 November 2013